Diffusion on the chaotic web of a Hamiltonian oscillator with incommensurate forcing

Gabor Schmera*
Department of Physics, University of Missouri at St. Louis, St. Louis, Missouri 63121

Peter Jung
Institut für Physik, Universität Augsburg, D-8900 Augsburg, Germany

Frank Moss
Department of Physics, University of Missouri at St. Louis, St. Louis, Missouri 63121
(Received 11 September 1991)

We show, with precision numerical experiments, that far enough from the origin, the phase space of a Hamiltonian oscillator, kicked at a frequency that is incommensurate with its natural frequency, is featureless at some level of precision; that is, the periodicities that lead to island chains in resonantly forced oscillators are strongly suppressed. Therefore this system is suitable for the study of high-dimensional analogies of chaos, such as Fokker-Planck dynamics and Einstein diffusion. We determine the diffusion constants and the probability densities numerically and compare them to previous theoretical predictions. We observe a crossover behavior of the diffusion constant between regions of weak and strong forcing.

PACS number(s): 05.45.+b, 05.20.−y

I. INTRODUCTION

The kicked Hamiltonian oscillator has long been studied as a nonrelativistic model of the motion of a charged particle in a magnetic field interacting with a transverse electromagnetic wave packet [1,2]. A widely used approximate equation of motion, valid when the interaction time of the wave packets is small compared to the natural period, or $\Delta/v_g \ll 2\pi/\omega$, is

$$\ddot{x}+\omega_0^2 x=\frac{e}{m}E_0\sin(kx)\sum_{n=0}^{\infty}\delta\left[t-n\left[\frac{2\pi}{\omega}\right]\right], \qquad (1)$$

where $\omega/\omega_0=q$ is the ratio of the rate at which the oscillator is kicked to the natural frequency. The phase space of this equation can be conveniently studied with the map representation

$$\begin{aligned} u_{n+1}&=(u_n+K\sin v_n)\cos\alpha+v_n\sin\alpha\ , \\ v_{n+1}&=-(u_n+K\sin v_n)\sin\alpha+v_n\cos\alpha \end{aligned} \qquad (2)$$

obtained by use of the dimensionless variables $u=k\dot{x}/\omega_0$ and $v=-kx$; where $\alpha=2\pi\omega_0/\omega$ and $K=2\pi(e/m)E_0k(1/\omega\omega_0)$ is the strength of the nonlinearity. Zaslavsky and his co-workers have extensively studied the structure of the phase space of this map for resonant kicking frequencies, that is, for ω/ω_0 an integer [1–3] as well as other Hamiltonian systems [4] and a higher-dimensional generalization [5]. They found a phase space composed of a tiling of islands which result from orders of the periodicities separated by a chaotic web of infinite extent. Thus two general types of motion are possible: trapped motion, which can be periodic, quasiperiodic, or chaotic, within the islands surrounded by undestroyed Kolmogorov-Arnold-Moser (KAM) surfaces; or unbounded, diffusivelike motion on the web.

Studies on diffusion in Hamiltonian systems are not new, dating back to Chirikov, who studied diffusion on the web of the standard map [6]. However, it is not clear that a satisfactory diffusion theory exists, and interest continues [7–9]. Recently, for example, Lichtenberg and Wood [8] have constructed an approximate theory of diffusion on the web of the map (2) for the resonant case (specifically for $q=4$) valid in the small-K region, which they then tested numerically. The starting point for this theory is the observation that the area preserving map (2) asymptotically fills the entire phase space. An important parameter is the ratio of the area in the space of the connected, chaotic web to that filled by the islands. For resonant forcing, and for $K \ll 1$, this ratio is also small compared to unity. The diffusive motion, consequently, takes place only along thin connected filaments. These are the remains of destroyed separatrices which lie between the (considerably larger) islands of periodic and quasiperiodic orbits. An example is shown in Fig. 1(a).

In this paper, we examine diffusion on the web of the map (2) in an extreme where the islands shrink to virtually zero measure leaving the web to occupy nearly the entire phase space. This is accomplished by incommensurately forcing of the oscillator with respect to its natural frequency. Under these conditions, and, as we show below, far enough from the origin, the angular measure of the map is uniform (to within some accuracy), while the radial measure mimics a time-evolving diffusive process. These observations are, of course, not new. Our interest is, however, to make precision determinations of the diffusion constants D, and the time-evolving probability densities, by carrying out an order of magnitude more iterations of the map at double precision than have previously, to the authors' knowledge, been reported. More-

over, we have observed the crossover between small-K and large-K diffusive behavior.

There is no *a priori* reason to suppose that the dynamics generated by any such map as (2) should be describable by infinite-dimensional tools such as the Fokker-Planck or diffusion equations, though the proposition has long fascinated dynamicists [10–15]. Continuing interest also stems from the fact that Hamiltonian systems such as (2) represent the classical limiting behavior of model quantum chaotic systems, where the "break time" marks a transition from quantum dynamical localization to classical diffusion [16–18]. The reason most often advanced for the high-dimensional behavior of classical Hamiltonian systems is the stochastic nature of scattering at the hyperbolic points which lie between the islands [19,20]. Presumably, numerical experiments on systems which have high densities of such points should then favor the observation of "statistical" or "thermodynamic" behavior. We show, with experiments based on 8×10^8 map iterations, that ideal diffusion is not more closely approximated with large numbers of iterations, even with incommensurate forcing which itself introduces disorder.

Our results can be summarized as follows: (1) we find that a set of initial points written to random locations within a thin annulus, and from which all periodic and quasiperiodic points were eliminated, diffuse radially outward while maintaining an approximately uniform angular measure so long as the annular region lies outside a certain small region surrounding the origin; (2) the process *approximately* follows Einstein's diffusion law [21] $\langle r^2\rangle \propto t$, where r is the distance from the origin, with the approximation becoming better for larger values of K; (3) the time-evolving measure in the radial coordinate can be described by a two-dimensional (cylindrical) diffusion equation; and finally, (4) the approximate diffusion law, D versus K, obtained by Lichtenberg and Wood is preserved in the limit of small K, while the Chirikov diffusion law applies in the region of large K with the crossover at $K\cong1$.

This short paper is organized as follows. In Sec. II we discuss our numerical routines, present the results, and compare them to the two theories. In Sec. III we present a simple calculation of the diffusion constant, valid for strong perturbation strength. In Sec. IV we summarize our results and comment on the accuracy of the present theories.

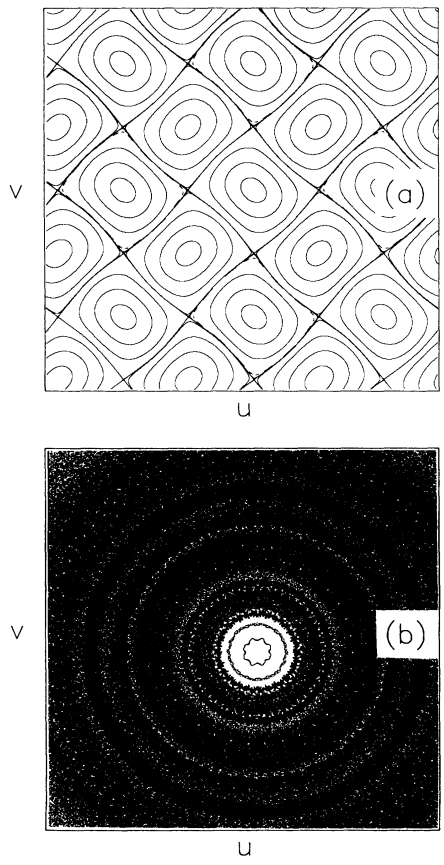

FIG. 1. (a) The web for resonant forcing, $\omega/\omega_0=4$, with $K=0.6$ as in the diffusion studies of Ref. [8]. The horizontal and vertical scales are ±10. (b) The web for irrational forcing, ω/ω_0 equal to the computed golden mean with $K=0.6$. The scales are ±150.

II. RESULTS

The numerical calculations were done on an Apollo DN10000 with two processors in 64-bit precision. A phase space portrait of the map (2) for resonant forcing with $\omega/\omega_0=4$ is shown in Fig. 1(a). The highly structured nature of the phase space, partitioned into island resonances bounded by a chaotic lattice of infinite extent (the web) is indicated by iterating individual trajectories originating on a grid of initial points. Lichtenberg and Wood [8] have studied diffusion for the resonant case on this web. By contrast, approximate incommensurate forcing was introduced by setting ω/ω_0 equal to the golden mean:

$$\frac{\omega}{\omega_0}=\frac{\sqrt{5}-1}{2}\ , \tag{3}$$

which computes as a rational because of the finite machine precision. A phase portrait, generated for all the same conditions (except for the scale of view) as used for the resonant case, is shown in Fig. 1(b). We note that, except near the origin, the structure has largely disappeared, being replaced by a more-or-less amorphous appearance which suggests random behavior. In fact, cantori, or island chains which are roughly circular in shape and centered on the origin, do remain, but as we move further from the origin they sink from view, falling below the level of the machine precision. Far enough from the origin, they are impossible to locate, and are therefore disregarded. The structure near the origin and the cantori are probably artifacts of the finite machine precision, in which case they represent high-order resonances due to the rationality of the computed value of the number (3).

Some of the nearer island chains have been located by computing the maximum Lyapunov exponent λ of a sequence of orbits originating on initial points on the u axis. The maximum exponents were obtained by stan-

dard techniques [22,23] and averaged over typically 10 000–100 000 iterations per orbit, depending on the strength of the forcing, K, until convergence to about 1 part in 10^4 was achieved. Figure 2(a) shows λ computed for irrational forcing and $K=0.6$ for each of 5000 initial points spaced at intervals $\Delta u=0.1$ on [0,500]. The occurrences $\lambda=0$ locate island chains which intersect the u axis and happen to fall on one of the initial points. The chains, while more numerous near the origin, persist at large distances from the origin. In contrast, Fig. 2(b) shows the same experiment carried out for the same conditions except for larger K. While the island chains are again more numerous near the origin, they become much less numerous beyond $u=100$ and are undetectable beyond $u=208$ up to a maximum distance of $u=8000$. The experiments we report here were carried out in the region beyond $u\cong 200$, where the diffusion process is not detectably influenced by the (hidden) island chains.

We have positioned a set of initial points written to random locations on a thin ($\Delta r=1$) annulus of radius $r=100$ centered on the origin, where r and θ are the polar coordinates, $r^2=u^2+v^2$ and $\theta=\tan^{-1}(v/u)$. For experiments with $K\leq 1.4$, the annulus contained a set of 8000 points, but for $K>1.4$ we only used 1000 points. The Lyapunov program was used to locate and eliminate all chance periodic and quasiperiodic points from the sets (which were replenished until they contained either 8000 or 1000 initial points on the web). Because the scale of the diffusion experiments described below was typically extended to $r\cong 8000$, therefore, when summed over θ, the density of the initial sets, located at $r=100$, could be considered effectively a δ function at the origin. Figure 3 shows the set of 1000 initial points on a horizontal scale of $r=1500$; (a) after 10^4 iterations, and (b) after 10^6 iterations, respectively. These results show two features: (1)

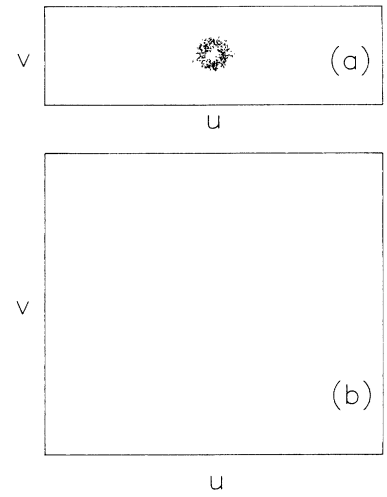

FIG. 3. Iterations on the $[u,v]$ plane of the set of 1000 initial points written to random locations on a thin annulus centered on the origin with a radius of $r=100$. The horizontal scales are ± 1500. (a) After 10^4 iterations, and (b) after 10^6 iterations of each point. $K=1.0$.

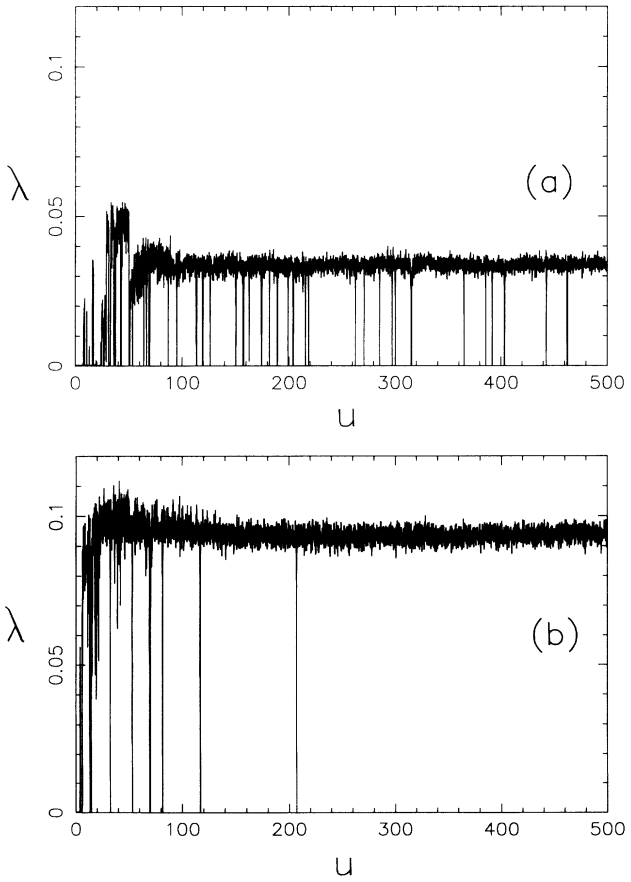

FIG. 2. (a) The Lyapunov exponents of the irrationally forced map from 5000 equally spaced initial points along the u axis for $K=0.6$. The zeros indicate the presence of periodic or quasiperiodic orbits which intersect the u axis and also happen to fall on one of the initial points. (b) The same plot except for $K=1.0$. Note that the periodic orbits lying further from the origin are suppressed.

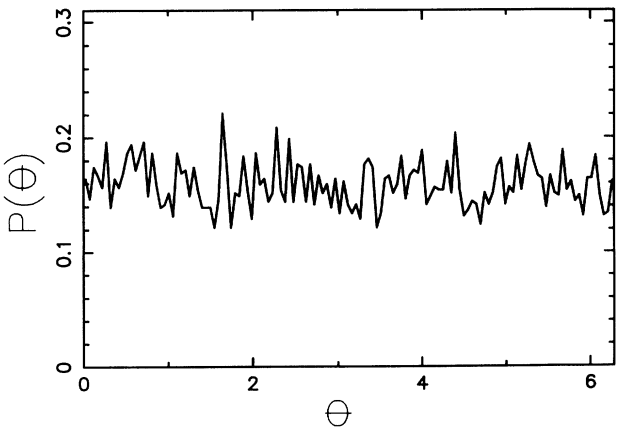

FIG. 4. The probability density of the angle θ, in radians, summed over all r for 8000 random initial points on the annulus, each point iterated 10^6 times. The density shows approximately equal probability on $[0,2\pi]$. $K=1.0$

diffusion in both radial and angular directions, and (2) the θ directions appear to preserve their random initial angles for all iterations. The latter observation supports the random phase approximation which is essential for the construction of diffusion theories [6,10].

In order to test the validity of the random phase approximation, we have measured the angular probability density $P(\theta)$ summed over all r for our 8000 initial point set iterated 10^6 times. The result is shown in Fig. 4, where we see that $P(\theta) \cong$ const, though a reasonable approximation, is in fact only an approximation, since some discernible structure exists. Note the expanded vertical scale. For comparison, we show in Fig. 5 a single orbit begun from an initial point near the origin but on the web. Figure 5(a) shows the orbit $r(n)$ and (b) shows the angular differences, $\Delta\theta = \theta_n - \theta_{n-1}$, between each pair of successive iterates. While $r(n)$ looks similar to a random walk process, the $\Delta\theta$ values are noticeably correlated. That is, while $P(\theta)$ is more-or-less uniformly distributed on $[0, 2\pi]$, there is a peaked distribution $P(\Delta\theta)$ unlike what would result from a random walker. The twist in the map persists even when incommensurately forced.

We now turn to the radial diffusion process. At each map iteration n, commencing with the initial point set ($n = 0$), we compute $\langle r^2 \rangle = (1/N) \sum_{j=1}^{N} r^2 j$, where $N = 8000$ or 1000 for small or large K, respectively, and plot this quantity versus n. The results are shown in Fig. 6(a) for small values of K and (b) for large values of K. The results are only approximately linear, as noted earlier by Chirikov for the standard map. Similar effects are evident in the data of Lichtenberg and Wood [8] for this map in the resonant case. In fact, the results systematically oscillate with long period (the "Chirikov oscillations") about a linear law. Chirikov has speculated that the oscillations are the result of weak, long-time correlations in θ. It is worth noting that the oscillations persist in our experiments which were done with 7000 more initial points and an order of magnitude more iterations than previous experiments. Figure 6(b) shows the results of iterating the smaller set of initial points for the larger range of K values. We have observed, as did Chirikov also, that the amplitude of the oscillations becomes smaller as K is increased, becoming virtually undetectable for $K > 10$. No oscillations are visible in Fig. 6(b), but the effect is masked by the larger fluctuations due to the smaller size of the initial point set. We have matched the data of Fig. 6 (as well as a number of additional such sets) to the diffusion law [21]

$$\langle r^2 \rangle = 4Dn \tag{4}$$

in order to obtain D for various values of K. The results are shown in Fig. 7. We note that evidently $D \propto K^3$ for small K, and $D \propto K^2$ for large K with the crossover being around $K \cong 2.5$. The straight lines depict these two be-

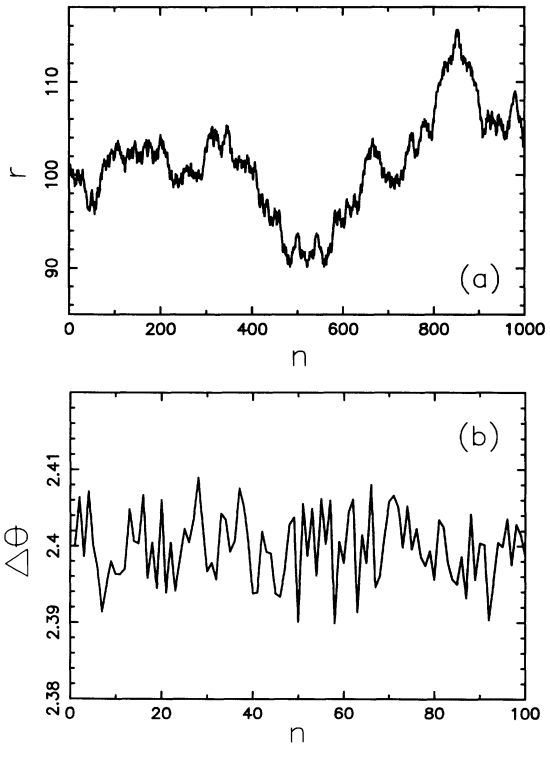

FIG. 5. (a) A single trajectory, $r(n)$, started on the connected web just beyond the last, visible, undestroyed KAM surface surrounding the origin. The scales are 150, and $K = 1.0$. (b) The change of the angle, $\Delta\theta$ in radians, between successive iterations vs the number of iterations n for the trajectory shown in (a). Note that the mean is approximately 2.4 radians.

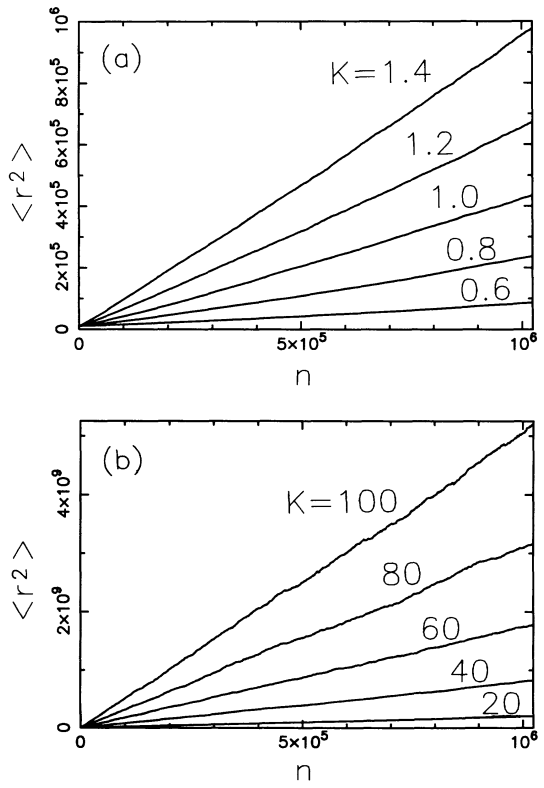

FIG. 6. The evolution of the mean square radii, (a) of the 8000 points in the small-K range, and (b) of the 1000 points in the large-K range. The slopes give the diffusion constants as shown by Eq. (4).

haviors. Chirikov has obtained the $D \propto K^2$ law as a rigorous result in the limit of large K for the standard map. Lichtenberg and Wood [8] find $D \propto K^3$ in the limit of small K is predicted by their approximate diffusion theory applied to the (thin) web of the resonantly forced map (2). The present results are thus consistent with the two theories and, moreover, show the details of the crossover behavior.

We turn now to the radial probability distributions $P(r)$ summed over all θ. These distributions are nonstationary since diffusion is radially outward from the vicinity of the origin. Figure 8 shows our results, for the set of 8000 initial points, for three values of n ranging to $n = 10^6$. Note that on this scale, where $r_{\max} = 2000$, the initial points at $r = 100$ would appear as a δ-like feature close to the origin. These results can be explained by a simple diffusion law

$$\frac{\partial P(r,\theta)}{\partial n} = D \nabla^2_{r,\theta} P(r,\theta) , \tag{5}$$

which has the (normalized) solution, assuming the initial state to be a δ function at the origin, and for $\lim_{r\to\infty} P = 0$,

$$P(r) = \frac{r}{2Dn} \exp\left[-\frac{r^2}{4Dn} \right] , \tag{6}$$

where we have eliminated θ based on the observation that $P(\theta) \cong$ const. This function is shown by the solid lines in Fig. 8, where we have used the values of D previously determined from fits to Eq. (4) of the data shown in Fig. 5. Since there are no adjustable constants, the goodness

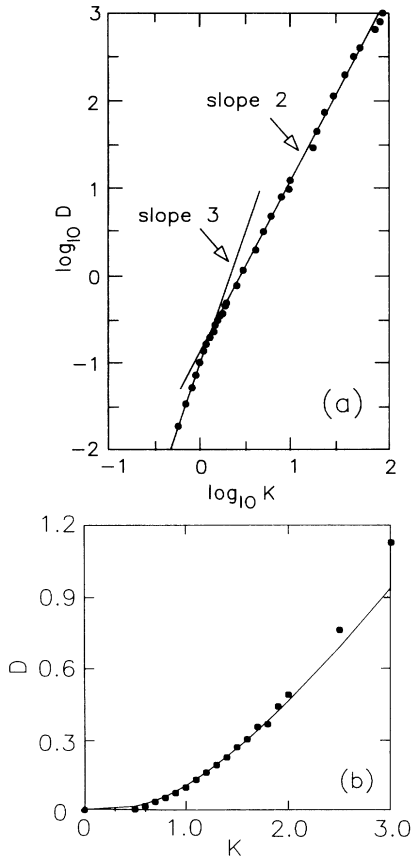

FIG. 7. The diffusion constant vs the forcing strength. (a) The crossover from $D \propto K^3$ (Lichtenberg and Wood behavior) to $D \propto K^2$ (Chirikov behavior) is shown. The solid lines indicate the slopes. (b) The theory of Lichtenberg and Wood (solid line) compared to the data in the small-K region plotted on a linear scale. Note that reasonably good agreement is obtained well into the crossover region.

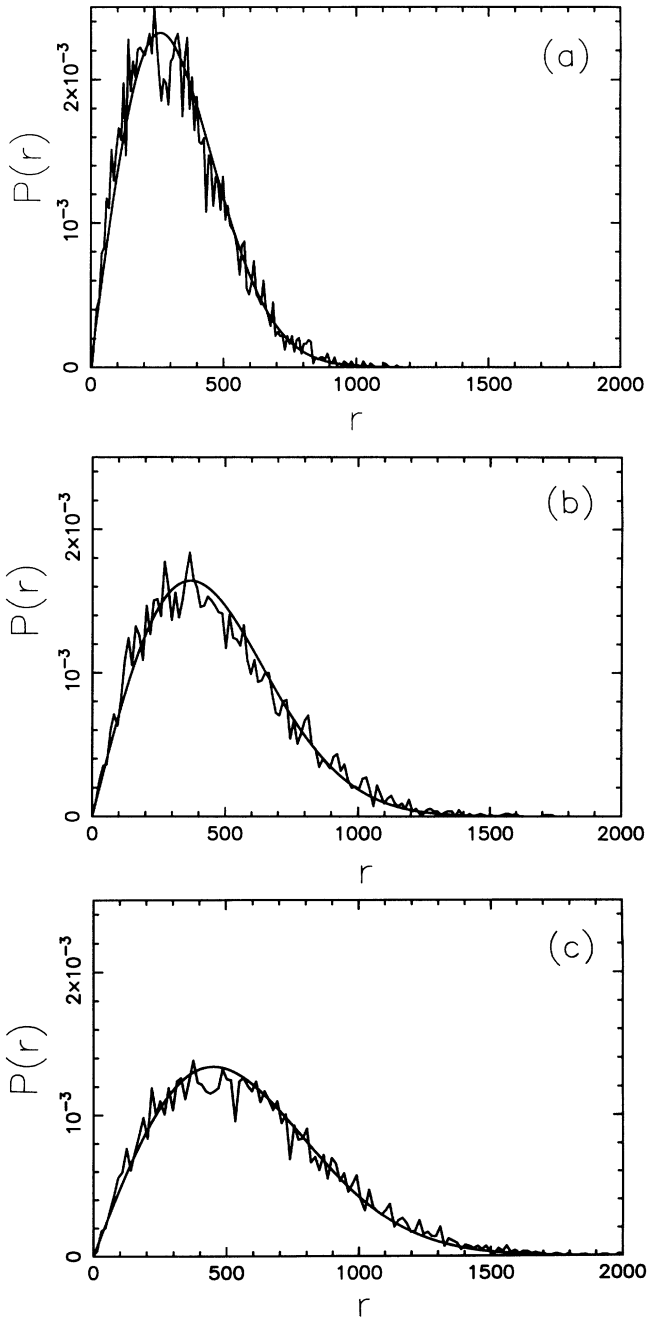

FIG. 8. Snapshot views of the evolution of the probability density of r summed over all angles for the 8000 initial points with $K = 1$. The solid lines are Eq. (6) with D taken from the slopes of the data shown in Fig. 6; (a) after $\frac{1}{3} \times 10^6$ iterations, (b) after $\frac{2}{3} \times 10^6$ iterations, and (c) after 1×10^6 iterations.

of the fit demonstrates the self-consistency of this approach. Moreover, this is a demonstration that ergodicity is a reasonably good approximation, since the second moment of r calculated from Eq. (6) yields exactly Eq. (4).

III. DIFFUSION COEFFICIENT FOR LARGE K

In this section, we present a rough estimate of the radial diffusion coefficient of the Zaslavsky map (2) for incommensurate forcing. Introducing the polar coordinates

$$r_n^2 \equiv u_n^2 + v_n^2 , \qquad \theta_n = \arctan(v_n / u_n) \tag{7}$$

the map (2) reads

$$r_{n+1}^2 = r_n^2 + K^2 \sin^2(r_n \sin\theta_n) + 2K r_n \cos\theta_n \sin(r_n \sin\theta_n) ,$$
$$\sin\theta_{n+1} = \frac{r_n \cos\alpha \sin\theta_n - [r_n \cos\theta_n + K \sin(r_n \sin\theta_n)] \sin\alpha}{[r_n^2 + K^2 \sin^2(r_n \sin\theta_n) + 2K r_n \cos\theta_n \sin(r_n \sin\theta_n)]^{1/2}} . \tag{8}$$

In the limit $K = 0$ (harmonic oscillator) the map (8) is reduced to

$$r_{n+1} = r_n , \qquad \theta_{n+1} = \theta_n - \alpha . \tag{9}$$

This is the motion on a circle which is densely covered for incommensurate forcing, $\alpha = 2\pi(\omega_0/\omega)$. From (9) we observe that the radial angle coordinates are the action-angle coordinates for the unperturbed system.

Considering an ensemble of trajectories, covering initially a circle of radius r_0, the ensemble-averaged radial map is obtained from (2) as

$$\langle r_{n+1}^2 \rangle = \langle r_n^2 \rangle + 2K^2 \sum_{l=1}^{\infty} J_{2l-1}^2(\langle r_n \rangle) , \tag{10}$$

where the $J_n(x)$ denote ordinary Bessel functions. Numerical evaluation of this equation results in diffusive behavior, that is, $\langle r_n^2 \rangle = 4nD$, where the diffusion coefficient D turns out to be a quadratic function of K as shown, for example, by the straight line of slope 2 in Fig. 7, or $D = cK^2$. The constant c can be estimated as follows: For large values of $\langle r_n \rangle / l$, we can substitute the asymptotic form of the Bessel functions, that is,

$$J_{2l-1}(\langle r_n \rangle) \cong \left[\frac{2}{\pi r_n}\right]^{1/2} \cos\left[\langle r_n \rangle + \frac{\pi}{4} - l\pi\right] \tag{11}$$

into (10). For $l > \frac{1}{4} e r_n$, the Bessel functions quickly decay to zero (for constant r_n) and those contributions can be neglected. We then obtain

$$\langle r_{n+1}^2 \rangle \cong \langle r_n^2 \rangle + K^2 \left[\frac{e}{\pi}\right] \cos^2\left[\langle r_n \rangle + \frac{\pi}{4}\right] , \tag{12}$$

where e is the base of the natural logarithms. For a given initial condition $\langle r_0 \rangle$, this map always approaches a fixed point. This is a consequence of the use of the asymptotic form of the Bessel functions, and can be cured by averaging the argument of the cosine term which is most sensitive to the initial conditions. This averaging yields

$$\langle r_{n+1}^2 \rangle = \langle r_n^2 \rangle + \frac{e}{2\pi} K^2 , \tag{13}$$

which is solved by (4) with

$$D(K) = \frac{e}{8\pi} K^2 . \tag{14}$$

Comparison of (14) with our numerical results for D shows quite good agreement as indicated in Table I, where we label the predictions of (14) by D_{analytic}. In fact, the ratio $D/D_{\text{analytic}} \cong 1.17$ over the whole range of D investigated, so that a reasonably good "working relation" for D would be

$$D(K) \cong 1.17 \left[\frac{e}{8\pi}\right] K^2 , \tag{15}$$

which plots over the straight line of slope 2 in Fig. 7.

IV. SUMMARY

We have presented the results of numerical diffusion experiments for the map often used by Zaslavsky, with resonant forcing, when approximately quasiperiodically driven. We have found, as have others previously using resonant forcing, that the evolution in time of the radial coordinate is approximately describable by a linear diffusion law. A simple two-dimensional diffusion equa-

TABLE I. Comparison of numerical and analytical values for D.

K	D	D_{analytic}
0.1	0.0014	0.001 08
0.5	0.032	0.027
1.0	0.127	0.108
2.0	0.505	0.532
3.0	1.14	0.973
4.0	2.02	1.73
5.0	3.16	2.70
7.0	6.22	5.29
10	12.7	10.8

tion yields time-dependent radial probability densities in approximate agreement with precision numerical experiments. Moreover, we have found our results for weak forcing to be in agreement with the diffusion theory of Lichtenberg and Wood, while for strong forcing they agree with a result due to Chirikov for the circle map. Moreover, we have provided an approximate calculation of D for large K for the Zaslavsky map, so that now analytic formulas exist which can be applied over the whole range of K for this map. We have observed that the accuracy of the small-K theory is good only for $K \lesssim 1.6$ while the large-K predictions are accurate beyond the crossover region up to the largest values of K ($\cong 100$) tested here.

ACKNOWLEDGMENTS

We are grateful to G. M. Zaslavsky, P. M. Koch, and Thomas Dittrich for enlightening discussions. This work was supported by the Office of Naval Research Grant No. N00014-90-J-1327, by NATO Grant No. 1272/90, and by the University of Missouri at St. Louis through its Visiting International Scholar program. P.J. thanks the Stiftung Volkswagenwerk for financial support. Some of the numerical results herein reported were checked on the Cray X/MP at the National Center for Supercomputing Applications at the University of Illinois–Champaign-Urbana.

*Present address: Naval Ocean Systems Center, Code 573, San Diego, CA 92152.

[1] M. A. Malkov and G. M. Zaslavsky, Phys. Lett. **106A**, 257 (1984).

[2] G. M. Zaslavsky, M. Yu. Zakharov, R. Z. Sagdeev, D. A. Usikov and A. A. Chernikov, Zh. Eksp. Teor. Fiz. **91**, 500 (1986) [Sov. Phys.—JETP **64**, 294 (1986)]; Pis'ma Zh. Eksp. Teor. Fiz. **44**, 7 (1986) [JETP Lett. **44**, 451 (1986)].

[3] A. A. Chernikov, R. Z. Sagdeev, D. A. Usikov, and G. M. Zaslavsky, Phys. Lett. A **59**, 1500 (1987).

[4] A. A. Chernikov, R. Z. Sagdeev, D. A. Usikov, M. Yu. Zakharov, and G. M. Zaslavsky, Nature (London) **326**, 559 (1987).

[5] G. M. Zaslavsky, in *Noise and Chaos in Nonlinear Dynamical Systems,* edited by F. Moss, L. A. Lugiato, and W. Schleich (Cambridge University Press, Cambridge, England, 1990), p. 289.

[6] B. V. Chirikov, Phys. Rep. **52**, 265 (1979).

[7] See, for example, H. Kook and J. D. Meiss, Phys. Rev. A **41**, 4143 (1990), and references therein.

[8] A. J. Lichtenberg and P. B. Wood, Phys. Rev. A **39**, 2153 (1989).

[9] J. H. Lowenstein, Phys. Rev. A **43**, 4104 (1991).

[10] A. J. Lichtenberg and M. A. Lieberman, *Regular and Stochastic Motion* (Springer-Verlag, New York, 1983), p. 286.

[11] V. I. Arnold and A. Avez, *Ergodic Problems of Classical Mechanics* (Benjamin, New York, 1968).

[12] G. M. Zaslavsky and B. V. Chirikov, Usp. Fiz. Nauk **105**, 3 (1971) [Sov. Phys.—Usp. **14**, 549 (1972)], a general review.

[13] J. Ford, *Transition from Analtyic Dynamics to Statistical Mechanics,* edited by I. Prigogine and S. A. Rice, Advances in Chemical Physics Vol. XXIV (Wiley, New York, 1973); *Lectures in Statistical Physics,* edited by W. C. Schieve and J. S. Turner, Lecture Notes in Physics Vol. 28 (Springer-Verlag, New York, 1974); *The Statistical Mechanics of Classical Analytic Dynamics,* Fundamental Problems of Statistical Mechanics Vol. 3, edited by E. G. D. Cohen (North-Holland, Amsterdam, 1975).

[14] G. M. Zaslavsky, *Chaos in Dynamic Systems* (Harwood, New York, 1985), Chap. 1.

[15] M. Falcioni, U. Marini Bettolo Marconi, and A. Vulpiani, Phys. Rev. A **44**, 2263 (1991).

[16] See, for example, these recent and excellent reviews: G. Casati and L. Molinari, Prog. Theor. Phys. Suppl. **98**, 287 (1989); T. Dittrich and R. Graham, Ann. Phys. (N.Y.) **200**, 363 (1990).

[17] P. M. Koch, Phys. Rev. A **43**, 4065 (1991), and references therein.

[18] G. Casati, B. V. Chirikov, D. L. Shepelyansky, and I. Guarneri, Phys. Rep. **154**, 77 (1987).

[19] G. A. Hedlund, Bull. Am. Math. Soc. **45**, 241 (1939).

[20] R. S. MacKay, J. D. Meiss, and I. C. Percival, Phys. Rev. Lett. **52**, 697 (1984); Physica **13D**, 55 (1984).

[21] A. Einstein, *Investigations on the Theory of the Brownian Movement* (Dover, New York, 1956), Chap. 2.

[22] A. Wolf, J. B. Swift, H. L. Swinney, and J. A. Vastano, Physica **16D**, 285 (1985).

[23] T. S. Parker and L. O. Chua, *Practical Numerical Algorithms for Chaotic Analysis* (Springer-Verlag, New York, 1989), Chap. 3.

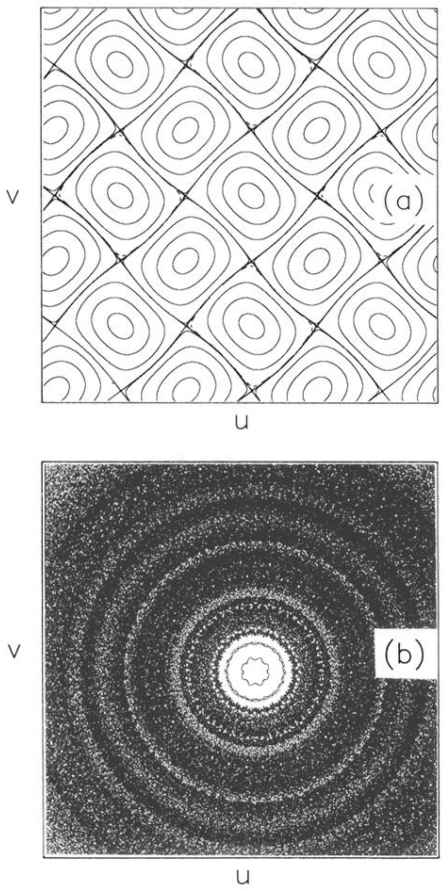

FIG. 1. (a) The web for resonant forcing, $\omega/\omega_0=4$, with $K=0.6$ as in the diffusion studies of Ref. [8]. The horizontal and vertical scales are ± 10. (b) The web for irrational forcing, ω/ω_0 equal to the computed golden mean with $K=0.6$. The scales are ± 150.